Available online at www.sciencedirect.com
ScienceDirect
Scripta Materialia 61 (2009) 951–954
Scripta MATERIALIA
www.elsevier.com/locate/scriptamat

On the hardness of shear bands in amorphous alloys

Byung-Gil Yoo,[a] Yong-Jae Kim,[a] Jun-Hak Oh,[a] U. Ramamurty[b] and Jae-il Jang[a,*]

[a] *Division of Materials Science and Engineering, Hanyang University, Seoul 133-791, Republic of Korea*
[b] *Department of Materials Engineering, Indian Institute of Science, Bangalore 560012, India*

Received 20 May 2009; revised 10 July 2009; accepted 29 July 2009
Available online 3 August 2009

The nanoindentation hardness of individual shear bands in a Zr-based metallic glass was investigated in order to obtain a better understanding of how shear band plasticity is influenced by non-crystalline defects. The results clearly showed that the shear band hardness in both as-cast and structurally relaxed samples is much lower than the respective hardness of undeformed region. Interestingly, inter-band matrix also exhibited lower hardness than undeformed region. The results are discussed in terms of the influence of structural state and the prevailing mechanism of plastic deformation.

Keywords: Bulk metallic glasses; Shear bands; Nanoindentation; Hardness

Shear transformation zones (STZs) and shear bands are the two main plastic deformation mechanisms in amorphous alloys [1,2]. STZs are the result of cooperative shearing of clusters of atoms (or molecules in the case of non-metallic glasses) and are common to all types of glasses. At high temperatures, they occur everywhere in the solid and hence flow is homogeneous. At low temperatures, relatively high stresses are required to activate them in sufficient number and strain tends to localize into narrow bands through their coalescence on planes of maximum shear. The bands, often referred to as shear bands, mediate plasticity in metallic glasses in an inhomogeneous manner [1].

An important concept that is often used as a measure of the structural disorder in amorphous alloys, especially in the particular context of plastic deformation, is the free volume [2,3]. STZs occur preferentially in locations where free volume is relatively high. Recent experimental results of micropillar compression of bulk metallic glasses (BMGs) by Dubach et al. [4] showed that the yield stress (i.e. the onset of plastic flow through shear band formation and propagation) of a BMG does not depend on the starting structural state of the BMG. Further, Volkert et al. [5] have pointed out that the global yield stress does not change with the deformation mode either—from shear-band-controlled heterogeneous deformation in larger specimens to STZ-mediated flow at small specimens.

What changes, however, is the free volume content within the BMG during plastic deformation. Since the operation of STZs requires local (and relatively large) dilatation, their operation enhances structural disorder within the amorphous structure of the metallic glass. This in turn makes the structure more readily amenable for subsequent plastic flow [6,7]. This was demonstrated by Bhowmick et al. [7] who employed the bonded interface technique to generate a large and well-defined plastic zone with profuse shear bands, which was subsequently probed by nanoindentation. Statistical analysis of the nanohardness data obtained from an extensively deformed region by Yoo et al. [8] showed that the deformed region is always softer than the undeformed region, despite the fact there is good probability of the nanoindent being made in the inter-band regions. The important questions that thus arise are: (i) what actually is the hardness of the shear bands; (ii) is the inter-band hardness similar or higher than that of the shear band; and (iii) how does the initial structural state influence these properties? Answers to these questions will help in furthering our understanding of plasticity in amorphous alloys, which is the purpose of this paper.

The investigated material is a Zr-based BMG, $Zr_{52.5}Cu_{17.9}Ni_{14.6}Al_{10}Ti_5$ (commercially designated as Vit 105). This BMG was examined in as-cast and annealed (at 630 K for 90 min) structural states. Because the annealing temperature is below the glass transition temperature (T_g) of the BMG ($\sim 0.93\,T_g$), structural

* Corresponding author. Tel.: +82 2 2220 0402; e-mail: jijang@hanyang.ac.kr

1359-6462/$ - see front matter © 2009 Acta Materialia Inc. Published by Elsevier Ltd. All rights reserved.
doi:10.1016/j.scriptamat.2009.07.037

relaxation occurs, which reduces the free volume in the BMG. No crystalline peak was detected in the X-ray diffraction spectra of the annealed specimen, as reported in our previous work [8].

The macroscale plastic deformation was introduced by high-load spherical indentation on the interface-bonded specimen. The details of the specimen preparation are described in Refs. [8,9]. The spherical indentations were performed with a peak load of 196 N and a loading rate of 5 μm s^{-1} using instrumented indentation equipment (AIS-2100, Frontics Inc., Seoul, Korea), with a 500 μm radius WC ball indenter. After indentation, the bonded interface was opened by dissolving the adhesive in acetone.

Although well-developed shear bands underneath the spherical indentation were obtained by the interface-bonding technique, it was difficult to directly measure the nanoindentation hardness of a narrow shear band due to the surface offset created by it. This is because a flat surface is essential for making accurate measurements, and this requires the surface steps to be removed by polishing. However, polishing makes it impossible to judge if the nanoindentation is made over a shear band or over the inter-band region. To overcome this difficulty, the following steps were adopted in the present work. First, one or two large Vickers indentation impressions were made on the deformed region by spherical indentation (see Fig. 1a) and imaged using scanning electron microscopy (SEM) (JSM-6330F, JEOL Ltd., Tokyo, Japan). Then, the surface was gently polished using 0.5 μm diamond paste.

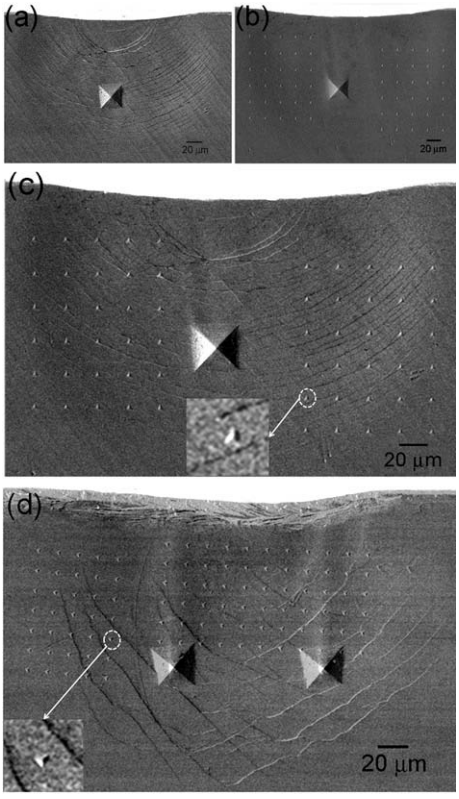

Figure 1. The SEM images showing the experimental sequence: (a) an image of the as-cast sample taken before nanoindentation and (b) after nanoindentation; (c) the image overlaying (a and b); (d) the overlaid image of the annealed sample. The inset images of (c and d) show the representative examples of the indentation made between shear bands, i.e. in the inter-band region.

A series of nanoindentation experiments were performed on the polished surface under a peak load of 50 mN and a strain rate of 0.05 s^{-1} using a Nanoindenter-XP (Nano Instruments, Oak Ridge, TN) with a Berkovich indenter. SEM images of the indented surface were then taken again (Fig. 1b). Because the Vickers indentation impression remained, essentially unaltered by the gentle polishing of deformed surface, the images taken before and after nanoindentation could be overlaid by making the images transparent in an image analysis program (see Fig. 1c for the as-cast sample and Fig. 1d for the annealed sample). This made it possible to estimate the precise location of the nanoindentation with respect to the shear band morphology underneath the spherical indent.

Figure 1c and d illustrate a clear difference in the size of the plastic zone (where shear bands were developed) and the shear band number density between as-cast and annealed sample; the latter exhibits a smaller deformed zone and a much higher inter-band spacing (and thus lower shear band density) than the as-cast sample. This means that the indentation-induced plasticity is limited in the annealed samples compared to that in the as-cast sample, which is a consequence of the reduced free volume in it [8,10,11].

The hardness data, measured on the deformed region, can be categorized into three groups according to the location of nanoindentation: (1) on the undeformed region (which is far away from subsurface deformation); (2) over the shear bands in the deformed region; and (3) between the shear bands in the deformed region (i.e. in the inter-band region which is representatively shown in the inset images of Figure 1c and d). Figure 2 shows the representative nanoindentation load–displacement (*P–h*) curves obtained from the three regions in the as-cast sample. While the indentation made in the undeformed region exhibits a smaller displacement at the peak load than those in the deformed regions, a distinct difference between the two deformed regions is also observed. The indentation made over shear bands shows a larger peak load displacement (i.e. softer) than that in the inter-band matrix.

All the three *P–h* curves show serrations (serial pop-ins), which have been related to the shear band nucleation and/or propagation during nanoindentation [1,8,12]. Among the three curves, the one obtained from the inter-band region shows the least pronounced serrations. As the shear banding activity is strongly dependent on the pre-existing initial free volume [10], this trend implies that the inter-band matrix in the deformed region may

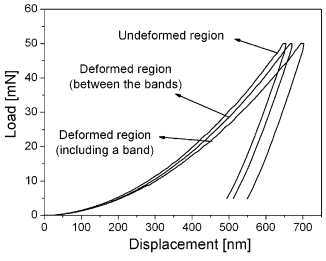

Figure 2. Load–displacement (*P–h*) curves obtained from three different regions.

have less free volume, whereas shear-banded regions have higher amounts of statistically distributed free volume.

The measured nanoindentation hardness values are summarized in Table 1. Note that the values were calculated according to the Oliver–Pharr method [13,14], which does not take the pile-up of material against the indenter (typically observed around the hardness impression of BMGs) into consideration and hence overestimates the hardness. As expected, the hardnesses of the deformed regions are smaller than those of the undeformed region, and the annealed sample shows much higher hardness than the as-cast sample. It is also clear that, for both as-cast and annealed samples, the hardness obtained from the deformed region between shear bands is higher than that from the deformed region, including shear bands. This indicates that the shear band itself may have lower hardness than the inter-band regime.

In order to calculate the hardness of individual shear bands from the hardness data in Table 1, we employed the simple rule of mixture:

$$H_{d-SB} = H_{SB}V_{SB} + H_{IB}V_{IB} \quad (1)$$

where H is the hardness and V is the volume fraction. The subscripts SB, d-SB and IB stand for shear band, the deformed region including shear bands, and the inter-band matrix region, respectively. To estimate the volume fraction of shear band (V_{SB}) in Eq. (1), it is necessary to consider the size of the indentation-induced plastic zone, which should be much larger than the triangular impression area. According to Johnson's expanding-cavity model for elastic–plastic indentation with a cone [15], the plastic zone radius (r_p) can be estimated as:

$$r_P = a\left\{\frac{1}{6(1-\nu)}\left[\frac{E}{\sigma_{YS}}\tan\beta + 4(1-2\nu)\right]\right\}^{1/3} \quad (2)$$

where a is the contact radius, β is the angle of inclination of the conical indenter to the surface, E is Young's modulus, ν is Poisson's ratio, and σ_{YS} is the yield strength. In order to relate this conical indentation model to the present results, we made the usual assumption that similar behavior is obtained when the angle of the cone gives the same area-to-depth relation as the pyramid. For the Berkovich indenter (whose centerline-to-face angle is 65.3°), the equivalent cone angle is 70.3° and thus β is 19.7°. Accordingly, by putting the values that were previously reported on the BMG with the same composition [16,17], $E = 89$ GPa, $\sigma_{YS} = 1.85$ GPa (from uniaxial compression test), $\nu = 0.37$, and the contact radius (determined by the Oliver–Pharr method [13,14]) into the right-hand term of Eq. (2), we could estimate the plastic zone size. The inset image of Figure 3 is an example to show how to calculate the volume fraction (V_{SB}) of shear band in the plastic zone: after drawing the estimated plastic zone on the SEM image and then on a reproduced black-and-white image, the V_{SB} was calculated using image analysis software. Note that the shape of the plastic zone is assumed to be a hemisphere according to Johnson's model [15]. The thickness of shear bands was in the range of 350–550 nm, and the average thickness was 460 nm. The calculated V_{SB} is summarized in Figure 3 which shows that it is ~13.4% and 10.4% for the as-cast and the annealed sample, respectively. Finally, nanoindentation hardness of the shear band itself was calculated by putting the measured hardness of each regime (H_{IB} and $H_{d\text{-}SB}$ in Table 1) and the calculated volume fractions of the shear band (V_{SB}) and the inter-band matrix (V_{IB}, which can be simply given as $1 - V_{SB}$) into Eq. (1). The result is also shown in Figure 3; the averaged shear band hardness was about 3.25 and 5.88 GPa for the as-cast and the annealed sample, respectively.

Table 1. Summary of the nanoindentation hardness.

	Deformed region (including a band) [GPa]	Deformed region (between the bands) [GPa]	Undeformed region [GPa]
As-cast	6.9 ± 0.14	7.5 ± 0.12	8.0 ± 0.11
Annealed	8.9 ± 0.17	9.3 ± 0.19	10.3 ± 0.35

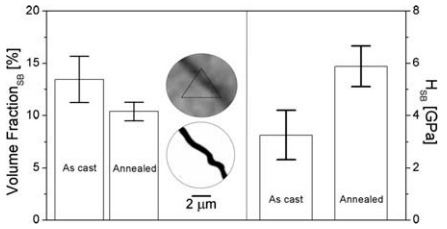

Figure 3. Volume fraction and hardness of shear bands in the as-cast and annealed samples.

In passing, it should be noted that Bei et al. [6] also estimated the shear band hardness of an as-cast BMG of the same composition and reported a value of 1.4 GPa, which is much lower than the value found in this work. This difference is possibly due to the following factors. Although Bei et al. [6] also applied a composite model (based on the rule-of-mixtures), they did not consider the fraction of shear bands in the indentation-induced plastic zone. Instead, they used the average ratio of shear band thickness (taken from the literature) to the inter-band spacing. More importantly, they did not take into account the softening of the inter-band matrix. Thus, their use of the hardness of undeformed matrix (instead of the softened inter-band matrix) in the rule-of-mixtures could cause an underestimation of shear band hardness for a given composite hardness. For instance, if the hardness of undeformed region (in Table 1) instead of H_{IB} is put into Eq. (1), the shear band hardness of the as-cast sample is measured as ~0.9 GPa. Other possible reasons are (i) different methods used to introduce the deformation (indentation vs. compression), which result in different levels of plastic strains; and (ii) different structural states of the glass despite the similarity in their compositions.

The results of the present work confirm that the amount of free volume is an important factor in determining the shear band hardness, as the trend of shear band hardness is in agreement (based on free volume theory) with the expectations that (i) shear bands have a higher density of free volume than undeformed matrix; and (ii) the as-cast sample has a larger amount of initial free volume than the annealed sample. Some experimental studies have been recently conducted to directly observe the structure of shear bands. By applying a quantitative

high-resolution transmission electron microscopy technique, Li et al. [18] and Jiang et al. [19] observed that much higher numbers of nanovoids (formed by condensed free volumes such as void formation due to vacancies in crystalline materials) were located in the interior of shear bands than in the surrounding matrix. Jiang et al. [19] argued, based on suggestions made by Wright et al. [20], that after removing applied stresses, excess free volume created during deformation tends to decrease by condensing into nanovoids, and the remaining excess free volume in shear bands (not merged into the voids), rather than the nanovoids, plays a more important role in the reduction in strength. Recently, Chen et al. [21] suggested that the nanovoids might be an artifact due to the different thicknesses of TEM foil specimens between the shear bands and undeformed matrix. Instead, they observed that shear bands have more free volume with a random configuration of atoms compared to that of the matrix, though the difference is small.

Our work also shows that it is not only the individual shear bands but also the inter-band matrix that have lower hardness than the undeformed matrix. It is possible that the lower hardness of the inter-band region is an experimental artifact caused by having a softer shear band close by and thus the "actual" hardness of the inter-band region (which is free from the influence of shear band) is the same as that of the undeformed region. To explore this possibility, we have examined the variation in the measured hardness with distance to the nearest shear band. Note that this analysis was possible only for the annealed sample in which the inter-band spacing is sufficiently large for a systematic analysis (see Fig. 1d). The result is shown in Figure 4. The measured hardness is almost constant at around 9.3 GPa (which is lower than ~10.3 GPa of the undeformed region: see Table 1) and does not vary significantly with the distance to the band. This result confirms that the inter-band region has indeed lower hardness than the undeformed region, which indicates that plastic deformation is not restricted to the shear bands alone [1]. This is because the STZs can operate everywhere within the plastic zone, and as a result the inter-band regions are softer than the completely undeformed region far away from the indentation impression. Since shear bands are manifestations of collective (and perhaps cooperative) avalanches of STZs along directions of maximum shear stress [22], it is possible that further structural modifications take place during their operation, which makes them more susceptible for plastic flow, leading to lower hardness than the inter-band regions.

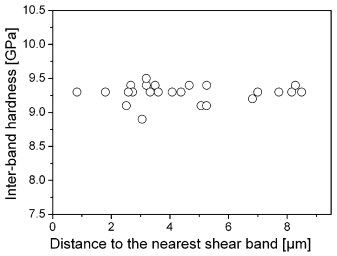

Figure 4. Variation in the measured inter-band hardness with a distance to the nearest shear band (for the annealed sample).

In summary, to better understand the role of non-crystalline defects in the phenomenological shear localization in amorphous alloy, the nanoindentation hardness of individual shear bands in a Zr-based BMG was investigated. The result convincingly showed that the hardness of the shear bands in the as-cast and the structurally relaxed samples is much lower than the respective hardness of undeformed region, which could be explained by the influence of structural state and the prevailing deformation mechanism. Interestingly, the deformed region between the shear bands also showed lower hardness than the undeformed region, indicating that plastic deformation is not restricted to the shear bands alone.

This research was supported partly by the Korea Science and Engineering Foundation (KOSEF) grant funded by MEST (Grant No. R01-2008-000-20778-0) and partly by the Korea Institute of Energy Technology Evaluation and Planning (KETEP) grant funded by MKE (Grant No. 2008-P-EP-HM-E-04-0000). One of the authors, U.R., acknowledges the financial support received for this work from the Department of Science and Technology, Government of India through a Swarna Jayanthi Fellowship. The authors thank Dr. H. Bei (at Oak Ridge National Laboratory) for providing the samples.

[1] C.A. Schuh, T.C. Hufnagel, U. Ramamurty, Acta Mater. 55 (2007) 4067.
[2] A.S. Argon, Acta Metall. 27 (1979) 47.
[3] F. Spaepen, Acta Metall. 25 (1977) 407.
[4] A. Dubach, R. Raghavan, J.F. Löffler, J. Michler, U. Ramamurty, Scripta Mater. 60 (2009) 567.
[5] C.A. Volkert, A. Donohue, F. Spaepen, J. Appl. Phys. 103 (2008) 083539.
[6] H. Bei, S. Xie, E.P. George, Phys. Rev. Lett. 96 (2006) 105503.
[7] R. Bhowmick, R. Raghavan, K. Chattopadhyay, U. Ramamurty, Acta Mater. 54 (2006) 4221.
[8] B.-G. Yoo, K.-W. Park, J.-C. Lee, U. Ramamurty, J.-I. Jang, J. Mater. Res. 24 (2009) 1405.
[9] B.-G. Yoo, J.-I. Jang, J. Phys. D Appl. Phys. 41 (2008) 074017.
[10] P. Murali, U. Ramamurty, Acta Mater. 53 (2005) 1467.
[11] U. Ramamurty, S. Jana, Y. Kawamura, K. Chattopadhyay, Acta Mater. 53 (2005) 705.
[12] J.-I. Jang, B.-G. Yoo, J.-Y. Kim, Appl. Phys. Lett. 90 (2007) 211906.
[13] W.C. Oliver, G.M. Pharr, J. Mater. Res. 7 (1992) 1564.
[14] W.C. Oliver, G.M. Pharr, J. Mater. Res. 19 (2004) 3.
[15] K.L. Johnson, J. Mech. Phys. Solids 18 (1970) 115.
[16] C.T. Liu, L. Heatherly, D.S. Easton, C.A. Carmichael, J.H. Schneibel, C.H. Chen, J.L. Wright, M.H. Yoo, J.A. Horton, A. Inoue, Metall. Mater. Trans. A 29 (1998) 1811.
[17] J.G. Wang, B.W. Choi, T.G. Nieh, C.T. Liu, J. Mater. Res. 15 (2000) 798.
[18] J. Li, Z.L. Wang, T.C. Hufnagel, Phys. Rev. B 65 (2002) 144201.
[19] W.H. Jiang, F.E. Pinkerton, M. Atzmon, Acta Mater. 53 (2005) 3469.
[20] W.J. Wright, T.C. Hufnagel, W.D. Nix, J. Appl. Phys. 93 (2003) 1432.
[21] Y.M. Chen, T. Ohkubo, T. Mukai, K. Hono, J. Mater. Res. 24 (2009) 1.
[22] E.R. Homer, C.A. Schuh, Acta Mater. 57 (2009) 2823.